Workability prediction for the Ampelmann A-type
a comparative study of different spectral wave models

by P. M. P. Bergmans

Student number:	4016084	
Project duration:	April 1, 2016 – February 14, 2017	
Thesis committee:	Prof. dr. ir. R. H. M. Huijsmans,	TU Delft
	Dr. ir. G. H. Keetels,	TU Delft
	Dr. ir. A. Vrijdag,	TU Delft
	Dr. ir. P. R. Wellens,	TU Delft
	Dr. ir. D. J. Cerda Salzmann,	Ampelmann Operations B.V.
	Ir. R. D. Schipperen,	Ampelmann Operations B.V.

Abstract

Clients of Ampelmann Operations B.V. require an indication of the workability when using an Ampelmann system. Overestimating workability can lead to reputation damage due to unexpected downtime, while underestimating workability weakens Ampelmann's value proposition. The predicted workability must be a close match to reality. Workability for the Ampelmann A-type is predicted using an in-house built prediction model, which contains several uncertainties regarding the modelling of waves. This research tests these uncertainties through several analyses.

Generated random wave phases possibly influence the consistency of workability prediction. Verification of prediction consistency shows that, due to the random wave phases, a small chance on incorrect results exists. However, as this possibility is minimal, it is considered not to limit this research. Deviations around the mean workability percentage are tested by evaluating 23 years of separate monthly and yearly wave scatter diagrams. The resulting deviations show large monthly variations and clear seasonal effects. These variations are weather dependent, thus beyond means of Ampelmann Operations B.V. to mitigate, and should be added as a disclaimer to clients.

Currently, the existence of a secondary sea system (swell) is excluded from the modelled wave spectra. In order to evaluate the influence of swell waves, a double peaked spectral model (Torsethaugen) is applied. Sensitivity of predicted workability is then tested to directional wave spreading and non-unidirectional wind sea and swell waves. Results show that accounting for swell within a generated wave spectrum influences workability significantly, especially when narrowing wave spreading and applying non-unidirectional swell.

The spectral wave models are then compared to a benchmark. The first comparison (wind sea dominated area) sets a benchmark by predicting workability using 37 years of 3-hourly detailed spectra (WaveWatch III). Before testing the earlier introduced spectral models, a 6 Parameter Based (6PB) model is introduced to approximate the detailed spectra, and test the effect of discarding spectral information. Comparable results have verified the 6PB model and indicate little influence of asymmetric spectral peaks, differences in 3-hourly wave spreading, and more than one swell system. The Torsethaugen model is then compared to the benchmark, showing a mismatch in predicted workability and created H_sT_z boundaries. Comparing the, by default applied, JONSWAP model shows similar results for this case study at a wind dominated area.

In this research, WaveWatch III data is available for a single location. To benchmark the spectral wave models at a swell dominated area, the verified 6PB model is used. The Torsethaugen model again results in a mismatch, which for that reason is considered unsuitable for Ampelmann workability prediction. The default JONSWAP leads to overestimated workability at this swell dominated area. As the current spectral model neglects the possibility of coexisting wind sea and swell waves, more detailed wave spectra (such as WaveWatch III or 6PB) are required to predict workability at swell dominated areas. These conclusions are based on results from the 6PB model, further verification of this model is recommended.

1 Introduction

Accessing offshore structures is a difficult task with constant motions due to waves. Using an Ampelmann[1] system to compensate wave induced motions allows safe personnel transfer at rougher sea conditions, resulting in an increase in workability. Clients of Ampelmann Operations B.V. require an indication of the workability prior to deploying an Ampelmann system. Overestimating the workability can lead to reputation damage for Ampelmann Operations B.V. due to unexpected downtime, while underestimating the workability weakens Ampelmann's value proposition and therefore its competitive position. As the predicted workability must be a close match to reality, the in-house built prediction model needs to represent the situation offshore accurately.

Predicting workability starts with modelling waves that represent the sea state at the area of interest. These waves are translated to vessel motions using the Response Amplitude Operator (RAO) of the host vessel.

Motions of the Ampelmann system are then derived from the vessel motions by using its location on deck and type-specific geometry. The final step compares the Ampelmann motions to type-specific limits and evaluates whether the situation is workable or non-workable, resulting in a workability percentage and boundary line. This boundary line represents the maximum workable combinations of significant wave height (H_s) and zero-crossing wave period (T_z).

This research focuses on the modelling of waves in combination with type-specific parameters of the Ampelmann A-type. Waves are generated by applying the Joint North Sea Wave Project (JONSWAP)[2] spectral model to each H_sT_z-combination within a given wave scatter diagram, after which the created spectrum is given a directional spreading. Furthermore, random wave phases are generated. These phases are necessary for the simulation of vessel time series.

There are several uncertainties regarding the workability prediction based on the current modelling of waves:

1. Introducing random wave phases could lead to inconsistencies in the statistical properties of the simulated vessel time series, if the chosen duration is too short
2. Wave scatter diagrams use averaged values, leading to a lack of insight into possible deviation around the resulting mean workability percentage
3. The default spectral model (JONSWAP) excludes the existence of a secondary sea system (swell) within the generated wave spectra, possibly leading to biased results
4. Sensitivity of predicted workability to the assumed directional spreading of wave spectra is unknown

In this paper these uncertainties are tested by several analyses.

- Verification of the consistency of an Ampelmann workability prediction
- Analysis of the deviation around a mean workability percentage
- Implementation of a double peaked spectral model to account for a secondary sea system when predicting workability
- Sensitivity analysis of predicted workability to directional spreading in wave spectra
- Comparison of the spectral wave models to a benchmark

Results presented in this paper are obtained from analyses using the RAO of the Damen PSV 1600. Two locations are considered: one dominated by a typical sea system of wind sea waves (Gemini wind farm), and the other typically dominated by swell waves (Baoab oil field). Using the RAO of a second vessel (Acta Orion) led to comparable results.

2 Verification of prediction consistency

If the duration of the simulation is too short, the introduction of random wave phases possibly leads to inconsistencies in the statistical properties of the simulated vessel time series. This can result in an incorrect workability prediction.

To verify prediction consistency, the duration of the simulated vessel time series is set on default (8000 seconds), and the workability prediction for a single situation (simulation settings and location) is repeated 385 times. The verification showed that the prediction is 99.3% consistent, which is based on a verdict with 95% confidence[3]. Although there is still a small chance of an incorrect workability prediction due to inconsistencies in time series, it is considered not limiting for the remaining analyses within this research.

3 Deviation around a mean workability percentage

The predicted workability represents a mean value for a year, season or month. To assess the use of a mean value to represent workability, the annual and monthly variations are researched. The monthly variations are analysed by taking separate wave scatters for each month of 23 years of wave data (3-hourly H_s and T_z values, retrieved from *waveclimate.com*[4]), instead of taking total averaged values.

This analysis showed large variations and clear seasonal effects. Figure 1 shows these results for the Gemini wind farm. In this example, the Standard Deviation (SD) varied from 4.59% (May) to 15.64% (January).

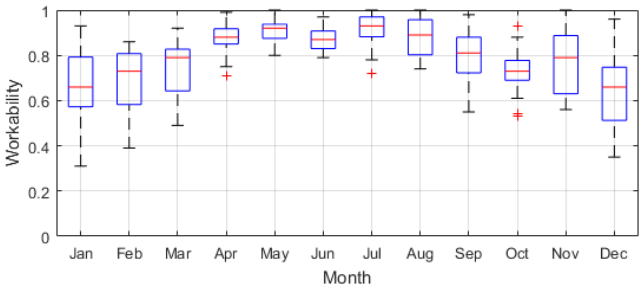

Figure 1: Large monthly variations in predicted workability at the Gemini wind farm, showing clear seasonal effects

Next to seasonal effects, the yearly deviations are evaluated. In this case, each of the 23 years has its own (average) wave scatter, which means seasonality is averaged out. Figure 2 shows the yearly workability of the 23 analysed years, with a boxplot displaying the deviations around a yearly mean. In the given example, the SD of a yearly prediction is equal to 4.15%.

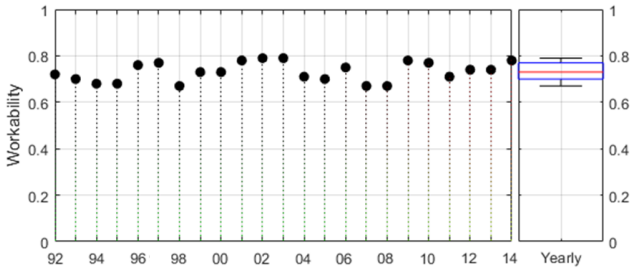

Figure 2: Yearly variations around the mean workability percentage at the Gemini wind farm

Results from this analysis are a side-note to this research, meant to provide insight and give context to other findings.

4 Double peaked spectral wave models

Before analysing the sensitivity of workability prediction to the directional spreading of generated wave spectra, alternative spectral models are introduced. The current prediction model uses either a JONSWAP (default) or a Pierson-Moskowitz[5] spectrum, both of which do not account for a secondary sea system (swell).

By implementing the most probable Ochi-Hubble[6] and simplified Torsethaugen[7] spectral models, it is possible to create double peaked wave spectra based on H_sT_z-combinations within a given wave scatter diagram. The Torsethaugen model creates spectra using both H_s and T_z, while the most probable Ochi-Hubble model only requires H_s as input. Figure 3 shows the four spectra ($S_\zeta(\omega)$) for $H_s = 2.5m$ and $T_z = 4.5s$, plotted against angular frequency.

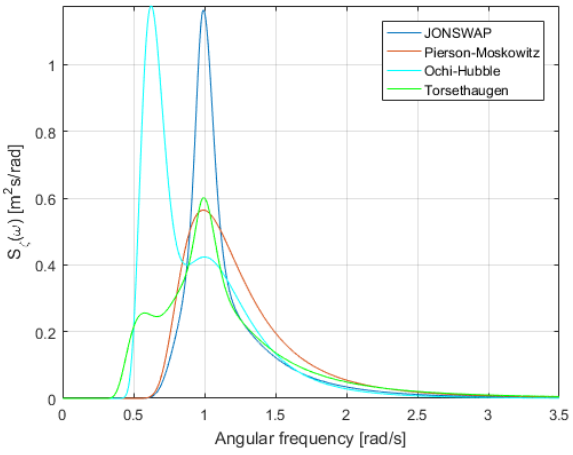

Figure 3: Double peaked versus single peaked spectral wave models, for $H_s = 2.5m$ and $T_z = 4.5s$

Applying these models to workability prediction shows a strong decrease in workability when using Ochi-Hubble and an increase when using the Torsethaugen model, with respect to the default prediction (JONSWAP). Workability is predicted for following waves ($\mu = 0°$) to head waves ($\mu = 180°$) in steps of 45°. Figure 4 shows the resulting workability. In this analysis, identical directional spreading (default) is applied to each generated spectrum.

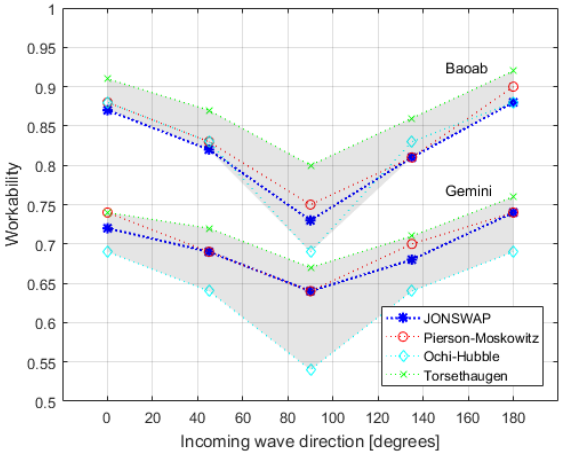

Figure 4: Predicted workability at the Gemini wind farm and Baoab oil field, using four different spectral wave models

To verify these alternative models, the significant wave height based on the zeroth-order spectral moment (H_{m_0}) is used. For a correct representation of a sea state, a spectral wave model should create a spectrum of which its total energy corresponds to the given input, meaning $H_{m_0} = H_s$. The zeroth-order spectral moment is calculated using equations 1 and 2 .

$$H_{m_0} = 4 \cdot \sqrt{m_0} \tag{1}$$

$$m_n = \int_0^\infty \omega^n \cdot S_\zeta(\omega) \cdot d\omega \tag{2}$$

The resulting H_{m_0} is compared to the H_s given as input for three different wave heights, displayed by table 1. Generated wave spectra, used to evaluate their H_{m_0}, are created with $T_z = 4.5s$.

	H_s [m]	1.25	2.50	5.00
H_{m_0} [m]	JONSWAP	1.22	2.44	4.88
	Pierson-Moskowitz	1.25	2.50	5.00
	Ochi-Hubble	1.46	2.88	5.56
	Torsethaugen	1.25	2.53	5.03

Table 1: Comparing H_{m_0} to the H_s given as input

The Ochi-Hubble spectrum in its most probable form overestimates the energy within the spectrum ($H_{m_0} > H_s$). Due to this overestimation and its independence of wave period, the most probable Ochi-Hubble spectral model is considered unsuitable for workability prediction. The Torsethaugen model is in accordance with the given input ($H_{m_0} \approx H_s$), and therefore is chosen as double peaked spectral model in the analysis of sensitivity to directional spreading. Although its H_{m_0} follows a given H_s, it does not mean the simplified Torsethaugen model is unquestionably applicable to workability prediction. The applicability of this model and an adjusted Ochi-Hubble model are discussed in section 6.

5 Sensitivity to directional wave spreading

Sensitivity to the directional wave spreading is tested by varying the spreading exponent and by testing the influence of non-unidirectional wind sea and swell waves. The sensitivity analysis is concluded with a note on the influence of the used RAOs.

Spreading exponent Spreading is added to the wave spectra by applying the $\cos^{2s}(\frac{1}{2}\mu)$ model[8], in formulae:

$$S_\zeta(\omega,\mu) = S_\zeta(\omega)\cdot D(\mu) \tag{3}$$

$$D(\mu) = A\cdot\cos^{2s}(\frac{1}{2}\mu) \tag{4}$$

$$A = \frac{\Gamma(s+1)}{\Gamma(s+\frac{1}{2})\cdot 2\sqrt{2}} \tag{5}$$

$S_\zeta(\omega,\mu)$	=	Directional wave spectrum	$[m^2s/rad]$
$S_\zeta(\omega)$	=	Wave spectrum	$[m^2s/rad]$
$D(\mu)$	=	Directional distribution	$[-]$
ω	=	Angular frequency	$[rad/s]$
μ	=	Incoming wave direction	$[deg]$
s	=	Spreading exponent	$[-]$
$\Gamma()$	=	The gamma function	$[-]$

Width of the directional spreading is determined by the value of the spreading exponent s, illustrated for five different s-values in figure 5.

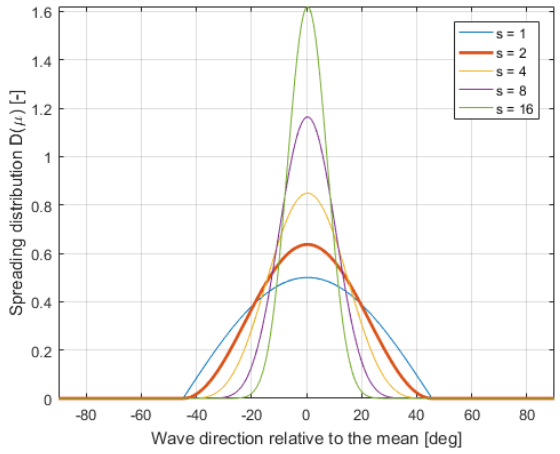

Figure 5: Spreading distribution D(μ) shown for five different s-values, using the $\cos^{2s}(\frac{1}{2}\mu)$ model

By default, Ampelmann workability studies are conducted using $s = 2$. Influence of the s-value is tested using JONSWAP spectra for five different incoming wave directions (μ), showing that narrowing wave spreading (higher s-value) for incoming waves corresponding to a sensitive part of the RAO (rolling motion at $\mu = 90°$) decreases workability drastically. Figures 6 and 7 show results at respectively the Gemini wind farm and the Baoab oil field.

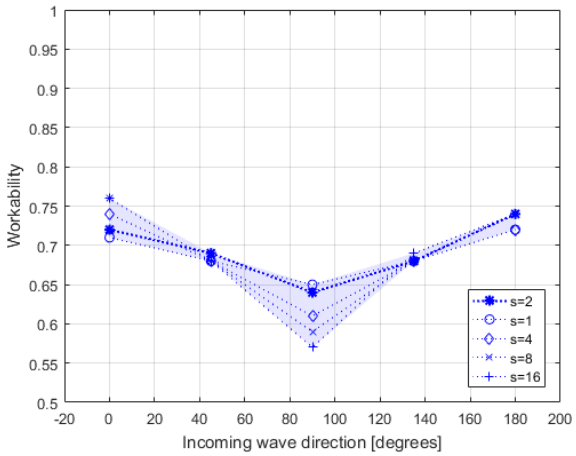

Figure 6: Sensitivity to s-values at the Gemini wind farm

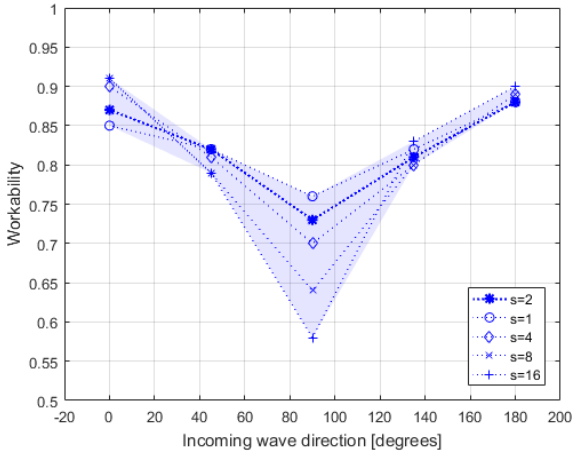

Figure 7: Sensitivity to s-values at the Baoab oil field

By splitting the spectral peaks created by the Torsethaugen model, it is possible to evaluate the effect of separate s-values for wind sea and swell. These effects are studied by varying the directional distribution per peak ($D_j(\mu)$) and combining the results, explained by equation 6. Indices 1 and 2 mark the separate sea systems.

$$S_\zeta^{TH}(\omega,\mu) = \sum_{j=1}^{2} S_\zeta^{TH,j}(\omega)\cdot D_j(\mu) \tag{6}$$

This separate wind sea and swell spreading showed a dominance of the spectral swell on the workability results. Results from this analysis are displayed in table 2.

Furthermore, a different number of discrete angles (N_μ) is applied to model the directional wave spreading. Results show that the chosen number of angles influences the prediction, especially for the combination of narrow wave spreading and a low number of discrete angles. Results seem to converge at $N_\mu \geq 24$, which is therefore recommended as the minimal quantity for modelling wave spreading.

		$s_{wind} = 2$		$s_{wind} = 16$	
	μ	Work.	$\Delta\%$	Work.	$\Delta\%$
$s_{swell} = 2$	180°	74%	Norm	74%	0
	135°	72%	Norm	72%	0
	90°	67%	Norm	64%	-4
	45°	71%	Norm	72%	1
	0°	76%	Norm	76%	0
$s_{swell} = 16$	180°	79%	7	79%	7
	135°	71%	-1	72%	0
	90°	61%	-9	58%	-13
	45°	72%	-1	72%	1
	0°	79%	4	79%	4

Table 2: Sensitivity to separate wind sea and swell spreading at the Gemini wind farm

Non-unidirectional wind sea and swell Non-unidirectional wind sea and swell waves are created by giving each spectral peak its own direction (μ_j), resulting in equation 7.

$$S_\zeta^{TH}(\omega, \mu) = \sum_{j=1}^{2} S_\zeta^{TH,j}(\omega) \cdot D_j(\mu_j) \tag{7}$$

Figure 8 shows an example of a non-unidirectional Torsethaugen spectrum for a sea state corresponding to $H_s = 2.5m$ and $T_z = 4.5s$, where separate spreading and directions are applied to the wind sea and swell peak ($s_{wind} = 2$, $s_{swell} = 16$, $\mu_{wind} = 135°$, and $\mu_{swell} = 270°$).

It is plausible that swell waves are more narrow spread than wind sea waves (due to the wave dispersion principle[9]), therefore a higher s-value is chosen to represent swell spreading. The different directions of figure 8 are randomly chosen to provide visual interpretation of non-unidirectional wind sea and swell within a wave spectrum.

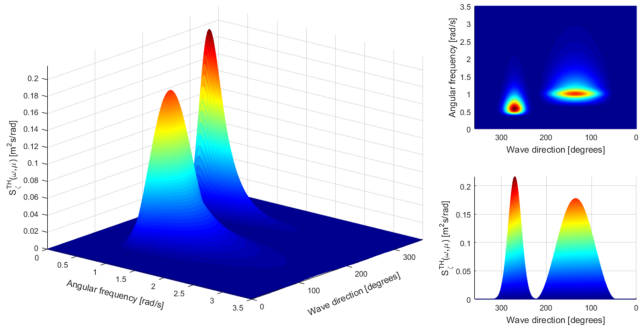

Figure 8: Directional Torsethaugen spectrum for $H_s = 2.5m$, $T_z = 4.5s$, $s_{wind} = 2$, $s_{swell} = 16$, $\mu_{wind} = 135°$, and $\mu_{swell} = 270°$

Sensitivity is tested by evaluating the effect on predicted workability when varying the incoming wave direction of the wind sea peak (μ_{wind}) and swell peak (μ_{swell}) in steps of 45°. Results are shown for fixed incoming wind sea head waves ($\mu_{wind} = 180°$).

	Gemini field		Baoab field	
μ_{swell}	Work.	$\Delta\%$	Work.	$\Delta\%$
180°	79%	Norm	94%	Norm
135°	72%	-9	90%	-4
90°	66%	-16	72%	-23
45°	72%	-9	90%	-4
0°	79%	0	94%	0

Table 3: Sensitivity to non-unidirectional swell waves, for $\mu_{wind} = 180°$, using $s_{wind} = 2$ and $s_{swell} = 16$

Non-unidirectional swell leads to considerable fluctuations in workability. Emphasizing the importance of accounting for swell waves when predicting workability. Occurrence of this non-unidirectionality is location dependent. To provide insight in the possibility of non-unidirectional swell waves at the Gemini wind farm and Baoab oil field, the probability density of μ_{swell} relative to μ_{wind} is plotted for both fields in figure 9 and 10.

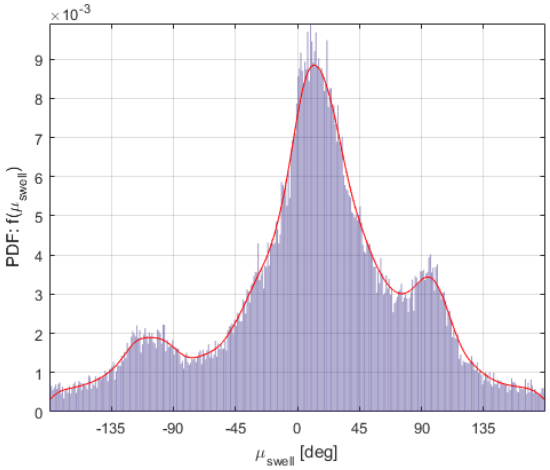

Figure 9: Probability density of μ_{swell} relative to μ_{wind} at the Gemini wind farm

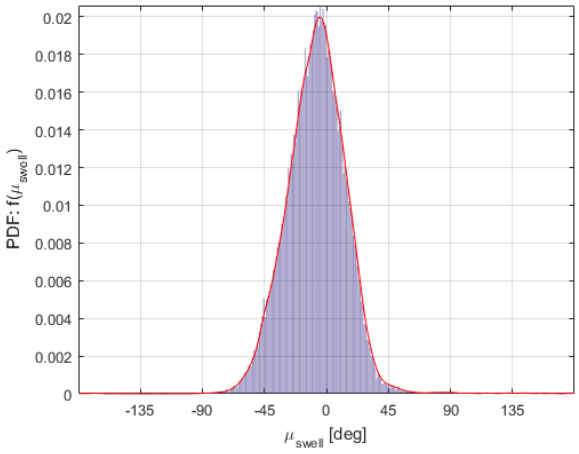

Figure 10: Probability density of μ_{swell} relative to μ_{wind} at the Baoab oil field

Influence of the RAO All results strongly depend on the RAO used in the analysis. The used RAO shows high sensitivity of rolling motion to low frequent excitation, which corresponds to swell waves.

Figure 11 shows the roll response of the Damen PSV 1600 for $\mu = 0°$ to $\mu = 180°$ in steps of 30°, where its resonance frequency is at 0.088 Hz (equal to a period of 11.4 seconds) and the highest response is found at incoming beam waves ($\mu = 90°$).

Due to the dominance of the used RAO in workability studies, further research on its influence is recommended.

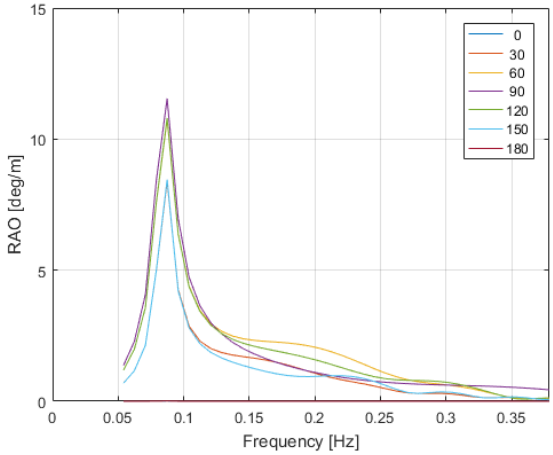

Figure 11: Roll response of the Damen PSV 1600

6 Comparison of spectral wave models

By comparing results of workability prediction using different wave spectra it is possible to determine whether the default JONSWAP method is applicable for workability prediction, and if other spectral models would provide more accurate results.

This comparison is executed in four steps, where at each step pieces of spectral information are discarded. First a benchmark is set (WaveWatch III), after which an approximation based on 6 parameters is introduced. The earlier discussed Torsethaugen model is then compared to the set benchmark, followed by the currently employed JONSWAP model.

(1) WaveWatch III A benchmark is set by determining workability using 37 years of 3-hourly WaveWatch III spectra for the Gemini wind farm, which are the most detailed spectra available (by courtesy of BMT Argoss[4]) to this research. Figure 12 shows an example of a WaveWatch III spectrum for the 8^{th} of June 1993 from 21:00 to 00:00, which corresponds to a sea state having $H_s = 0.34m$ and $T_z = 2.18s$.

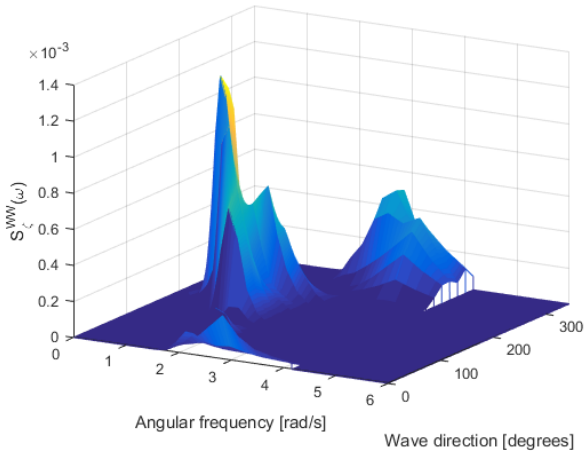

Figure 12: Example of a WaveWatch III spectrum, corresponding to a sea state of $H_s = 0.34m$ and $T_z = 2.18s$

Results show that, when presenting workability using H_sT_z-combinations, an overlap in workable and non-workable H_sT_z-combinations exists. This overlap is displayed in figure 16, where results of all the used spectral models are compared. Possible causes for this overlap are asymmetric spectral peaks, differences in 3-hourly wave spreading, the presence of one or more swell systems, ratio differences in $H_{s,j}$ and $T_{p,j}$, and non-unidirectionality of wind sea and swell waves.

(2) 6 parameter double peaked The WaveWatch III spectra are approximated by introducing the 6 Parameter Based (6PB) spectral model. This model is an adjustment of the Ochi-Hubble spectral model to create wave period dependency and normalising it to ensure that its H_{m_0} equals the H_s given as input, thus mitigating shortcomings of the earlier introduced most probable Ochi-Hubble model. Equations 8 to 14 show the formulation of the 6PB model.

$$S_\zeta^{6PB}(\omega,\mu) = nf \cdot S_\zeta^{aOH}(\omega,\mu) \tag{8}$$

$$\begin{aligned} S_\zeta^{6PB}(\omega,\mu) &= \text{6 Parameter Based spectrum} \\ S_\zeta^{aOH}(\omega,\mu) &= \text{Adjusted Ochi-Hubble spectrum} \\ nf &= \text{Normalisation factor} \\ \omega &= \text{Angular frequency} \end{aligned}$$

In which $S_\zeta^{6PB}(\omega,\mu)$ and $S_\zeta^{aOH}(\omega,\mu)$ are given in m^2/rad, and ω in rad/s.

The adjusted Ochi-Hubble spectrum is a summation of separate wind sea and swell peaks, where each peak has its own significant wave height ($H_{s,j}$), peak period ($T_{p,j}$), and mean wave direction (μ_j).

$$S_\zeta^{aOH}(\omega,\mu) = \sum_{j=1}^{2} S_\zeta^{aOH,j}(\omega) \cdot D_j(\mu_j) \tag{9}$$

$$\begin{aligned} S_\zeta^{aOH,j}(\omega) = \left(\frac{1}{2\pi}\right) \frac{H_{s,j}^2 T_{p,j}(\lambda_j + 0.25)^{\lambda_j}}{4\Gamma(\lambda_j)(T_{p,j}\frac{\omega}{2\pi})^{(4\lambda_j+1)}} \cdot \dots \\ \dots \exp\left\{-\frac{(\lambda_j + 0.25)}{(T_{p,j}\frac{\omega}{2\pi})^4}\right\} \quad \text{for} \quad j = 1,2 \end{aligned} \tag{10}$$

$$j = \begin{cases} 1 & \text{Swell sea system} \\ 2 & \text{Wind sea system} \end{cases}$$

The most probable Ochi-Hubble shape parameters (λ_j) are applied in this model.

The normalisation factor is equal to the ratio between the required zeroth-order spectral moment ($m_0^{H_s}$) and the zeroth-order moment of the adjusted Ochi-Hubble spectrum (m_0^{aOH}).

$$nf = \frac{m_0^{H_s}}{m_0^{aOH}} \tag{11}$$

$$m_0^{aOH} = \int_0^{\infty} S_\zeta^{aOH}(\omega) \cdot d\omega \tag{12}$$

$$m_0^{H_s} = \frac{H_s^2}{16} \tag{13}$$

$$H_s = \sqrt{H_{s,wind}^2 + H_{s,swell}^2} \tag{14}$$

Separate wind sea and swell spreading is applied by using mean s-values for the Gemini wind farm, retrieved from analysis of the WaveWatch III data:

$$\begin{aligned} s_{wind} &= 5.59 \\ s_{swell} &= 10.81 \end{aligned}$$

Figure 13 shows the resulting 6PB spectrum, which approximates the WaveWatch III spectrum of figure 12.

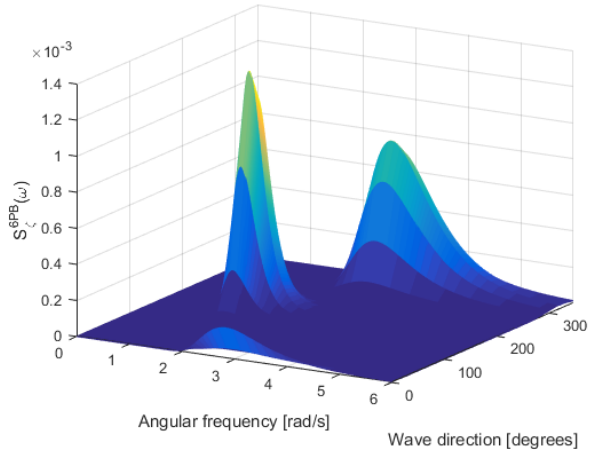

Figure 13: 6 Parameter Based spectrum, corresponding to a sea state of $H_s = 0.34m$, $T_z = 2.18s$, $s_{wind} = 5.59$ and $s_{swell} = 10.81$

The 6PB spectra are a close match with the detailed WaveWatch III spectra. Results using two different RAOs (Damen PSV 1600 and Acta Orion) showed matching results in 96.79% and 98.10% of all 3-hourly cases (37 years of data), resulting in a maximum of less than 1% difference in workability.

For this particular case study (the wind sea dominated Gemini wind farm), asymmetric spectral peaks, 3-hourly wave spreading differences and multiple swell systems have little influence on workability prediction. Furthermore, the close agreement with the WaveWatch III data verifies the 6PB spectral model. Figure 17 shows the workability H_sT_z-scatter of the Damen PSV 1600 at the Gemini wind farm when using 6PB spectra.

(3) 2 parameter double peaked The third step compares results from analysis using WaveWatch III spectra with the earlier introduced 2 parameter double peaked Torsethaugen model, illustrated by figure 14.

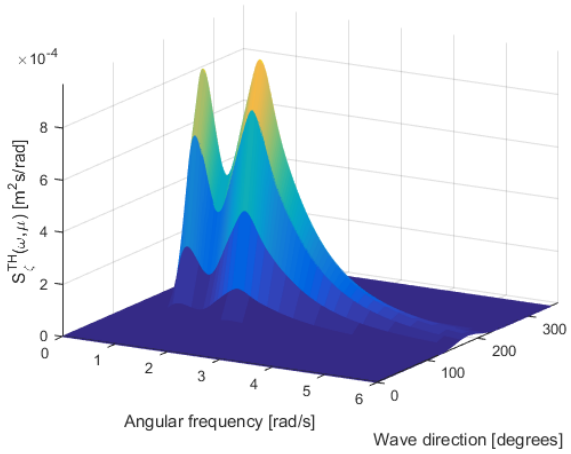

Figure 14: Torsethaugen spectrum, using $H_s = 0.34m$, $T_z = 2.18s$, $s_{wind} = 5.59$ and $s_{swell} = 10.81$

Boundary lines are drawn using the Torsethaugen model for $\mu_{swell} = 180°$ (upper limit) and $\mu_{swell} = 90°$ (lower limit), while keeping μ_{wind} fixed at 180°. Figure 16 shows the resulting Torsethaugen boundary lines.

This method creates insight in overlap between workable and non-workable H_sT_z-combinations due to non-unidirectional swell. The resulting representation of overlap is a mismatch with results that followed from WaveWatch III and 6PB analyses. This means either separate wind sea and swell wave heights and periods are needed, or the model is (in this case study) unsuitable for application of workability prediction.

(4) 2 parameter single peaked The final step is the comparison with the 2 parameter single peaked JONSWAP model. This step is executed using mean wave spreading for the Gemini wind farm, and default spreading ($s = 2$). The mean wave spreading is derived from the WaveWatch III data, and is equal to $s = 4.70$ for combined wind sea and swell systems. Figure 15 shows the directional JONSWAP with mean directional wave spreading applied for the same combination of H_s and T_z as the earlier showcased examples.

Comparing the JONSWAP method to the WaveWatch III results (figure 16) shows that a boundary line created with JONSWAP spectra is a fair approximation, especially when using mean wave spreading (JS mean). The resulting workability percentages are similar to analyses with WaveWatch III spectra.

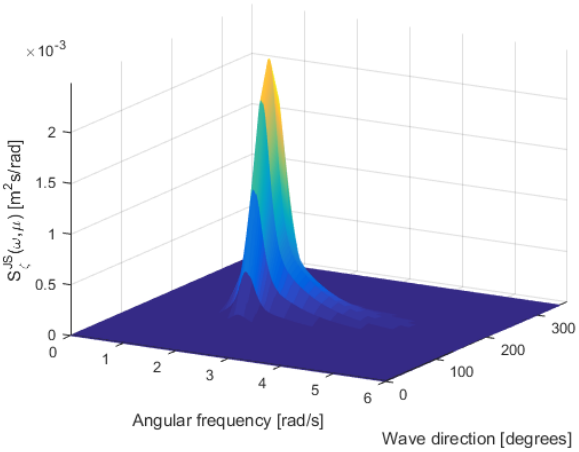

Figure 15: JONSWAP spectrum, using $H_s = 0.34m$, $T_z = 2.18s$, and $s = 4.70$

Overview of results A comparison of WaveWatch III, Torsethaugen, and JONSWAP analyses is shown in figure 16. Results from the 6PB analysis are shown in figure 17, where the default JONSWAP boundary line is merely drawn to simplify comparison with figure 16.

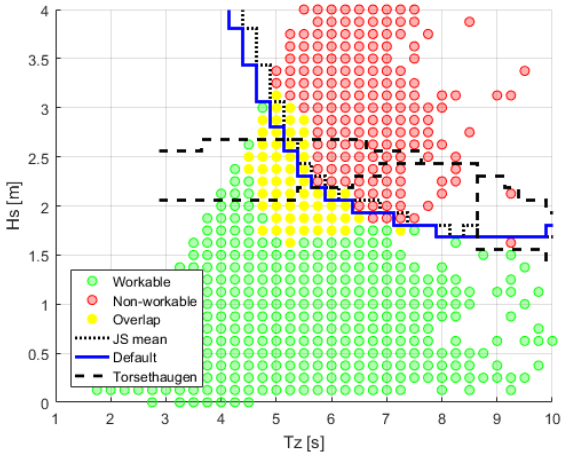

Figure 16: Comparison of results from analyses with WaveWatch III, Torsethaugen, and JONSWAP

Table 4 summarizes the resulting workability of the different methods of spectral modelling. The differences (normalised) with respect to the outcome of the WaveWatch III analysis are shown in the second column.

Method	Work.	Δ%
WaveWatch III	82.25%	Norm
6 Parameter Based	81.36%	-1
Torsethaugen $\mu_{swell} = 180°$	84.81%	3
Torsethaugen $\mu_{swell} = 90°$	72.96%	-11
JONSWAP mean spreading	82.23%	0
Default Ampelmann prediction	80.76%	-2

Table 4: Comparison of resulting workability at the Gemini field, differences normalised to WaveWatch III

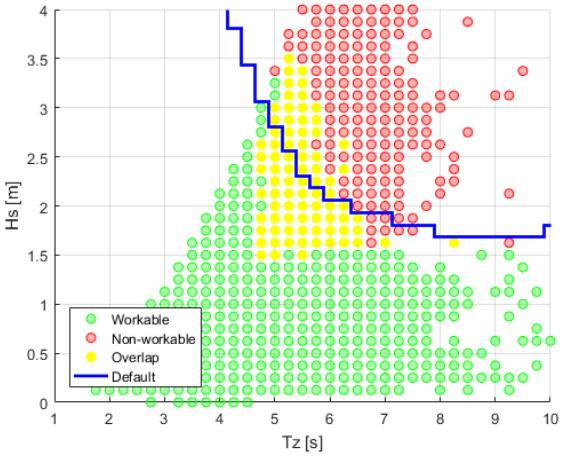

Figure 17: Results from 6PB analysis, showing the default JONSWAP boundary line as a reference

Case study of a swell dominated area Previous results are based on a case study using a wind dominated area, which could explain the close agreement between WaveWatch III and JONSWAP results. To evaluate this possibility, a second case study is executed, which evaluates the performance of the spectral models in a swell dominated area (Baoab oil field).

Unfortunately, for this swell dominated area there are no WaveWatch III spectra available to this research. In this case study the 6PB model is used as a benchmark, which creates the overlap in workable and non-workable H_sT_z-combinations. The 6PB model is applied to 23 years of 3-hourly wave parameters of the Baoab oil field, retrieved from *waveclimate.com*.

Results show (figure 18) that the Torsethaugen model again results in a mismatch with more detailed spectra, and therefore is considered unsuitable for Ampelmann workability predictions. The boundaries created with JONSWAP spectra follow the trend of the workable and non-workable H_sT_z overlap, but nonetheless result in an overestimation of the workability.

Table 5 displays the resulting workability from the different analyses at this swell dominated area.

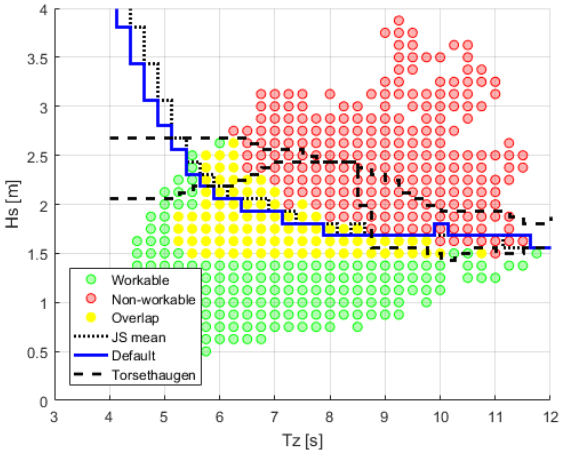

Figure 18: Comparison of spectral wave models at the swell dominated Baoab oil field

Method	Work.	Δ%
WaveWatch III	n/a	n/a
6 Parameter Based	84.25%	Norm
Torsethaugen $\mu_{swell} = 180°$	98.43%	17
Torsethaugen $\mu_{swell} = 90°$	96.05%	14
JONSWAP mean spreading	90.81%	8
Default Ampelmann prediction	88.98%	6

Table 5: Comparison of resulting workability at the Baoab field, differences normalised to 6PB

7 Conclusions

Based on the analyses within this paper, the following is concluded:

- The current workability prediction is 99.3% consistent (confidence of 95%), and therefore allows for a small possibility of an incorrect workability prediction due to inconsistencies in time series.
- Deviations around mean Ampelmann workability predictions differ per location and month(s) of interest. When communicating a workability percentage to clients a disclaimer must be added, as these variations are beyond means of Ampelmann Operations B.V. to mitigate.
- Narrowing wave spreading (higher s-values) for incoming waves at a sensitive part of the RAO decreases workability drastically. Applying separate directions and spreading to wind sea and swell waves leads to considerable fluctuations in resulting workability. All sensitivity strongly depends on the RAOs used in the analysis.
- Using WaveWatch III (and 6PB) spectra provides insight into the possible overlap between workable and non-workable H_sT_z-combinations.
- The 6PB model is a satisfactory fit to generate wave spectra when comparing it to the detailed WaveWatch III spectra, thus applicable to other areas.
- The simplified Torsethaugen model is unsuitable for Ampelmann workability prediction, as its results are a mismatch with the more detailed models.
- For wind sea dominated areas the Ampelmann approach using JONSWAP spectra is a fair approximation of the workability percentage. However, it lacks the insight of possible overlap between workable and non-workable H_sT_z-combinations. For swell dominated areas Ampelmann workability predictions are likely to overestimate the workability. To accurately predict workability for swell dominated areas, more detailed models, such as WaveWatch III or 6PB, are required.

8 Recommendations

Following from the presented analyses and conclusions, several recommendations are drawn:

- It is advised to investigate if it is achievable to complete workability studies without making use of time series, by performing all simulations in the frequency domain. Besides eliminating the (small) possibility of inconsistencies, it would decrease computational time. Lowering computational time increases feasibility of more detailed spectral analyses such as WaveWatch III or 6PB.
- Showing deviations around the mean workability percentage by using SD values per month depends on the area of interest. Ampelmann systems are operational worldwide, therefore multiple locations should be analysed. When performing these analyses, it is suggested to create a situation where the resulting workability does not reach the limits of 0% and 100%.
- Verification of four different spectral models showed discrepancies between H_{m_0} and H_s. A generated spectrum must be a correct representation of a sea state, therefore it is recommended to apply scaling within the prediction model to ensure H_{m_0} is equal to H_s.
- This thesis showed significant influence of non-unidirectional wind sea and swell waves. It is possible that an optimal vessel position exists when this non-unidirectionality is present. Further research on such a position could improve the workability of future projects.
- It is recommended to investigate the modelling error due to the chosen number of discrete angles (N_μ) to model wave spreading. This error is possibly related to the interpolation of the RAO, which should be examined.
- The extent of influence due to non-unidirectional swell waves can be examined by downscaling the 6PB model to a 4 Parameter Based (4PB) model, discarding the independent directions (μ_j). Evaluation of workability results with such a 4PB model could provide useful insights.
- In this thesis the verification of the 6PB model is based on a single case study using WaveWatch III spectra of a wind sea dominated area as a reference. Further verification is recommended, using areas with increasing dominance of swell waves. If further verification would result in a mismatch, it is advised to investigate the influence of multiple swell systems. This can be performed by expanding the 6PB model to a 9 Parameter Based model (9PB), which is allowable due to the implemented scaling. For a 9PB model, parameters of three different partitions are required.

Acknowledgements

I would like to thank Ampelmann Operations B.V. for sponsoring this research and providing its interesting and challenging subject. Furthermore, many thanks to my supervisors (thesis committee) from Ampelmann and Delft University of Technology for their guidance throughout the entire project. Finally, my family and friends for their support along the way.

References

[1] D. J. Cerda Salzmann, *Development of the Access System for Offshore Wind Turbines*. ISBN 9789088911941, 2010.

[2] K. Hasselmann et al., *Measurements of Wind-Wave Growth and Swell Decay during the Joint North Sea Wave Project (JONSWAP)*. Ergnzungsheft zur Deutschen Hydrographischen Zeitschrift Reihe, 1973.

[3] C. Lessard et al., *Project Management for Engineering Design*. ISBN 9781598291742, 2007.

[4] J. Vroom et al., *Wave spectra and partitions for a location in the North Sea*. BMT Argoss (unpublished), 2016.

[5] W. J. Pierson et al., *A proposed spectral form for fully developed wind seas based on the similarity theory of S. A. Kitaigorodskii*. Technical Report Prepared for U.S. Naval Oceanographic Office, 1963.

[6] M. K. Ochi et al., *Six-parameter wave spectra*. Proceedings of the 15^{th} International Conference on Coastal Engineering, 1976.

[7] K. Torsethaugen et al., *Simplified double peak spectral model for ocean waves*. Proceedings of the 14^{th} International Offshore and Polar Engineering Conference, 2004.

[8] H. Mitsuyasu et al., *Observations of the directional spectrum of ocean waves using a cloverleaf buoy*. Journal of Physical Oceanography, 1975.

[9] L. H. Holthuijsen, *Waves in Oceanic and Coastal Waters*. Cambridge University Press ISBN 9780521860284, 2007.